

Information theory rules out the reflex-chain model of *C. elegans* locomotion

John Webb and Saul Kato

Department of Neurology; Weill Institute for Neurosciences; Kavli Institute for Fundamental Neuroscience; and Center for Integrative Neuroscience, University of California, San Francisco, San Francisco, CA, USA

This manuscript was compiled on February 1, 2022

1 Despite decades of research, whether the *C. elegans* traveling-wave sinusoidal body pattern during locomotion is produced (a) by the undulations of the head followed by wave propagation down the body, or (b) via centrally coordinated posture control along the body, is still under debate. By studying relationships between the time series of postural angles along the body extracted from videos of moving worms, we find that the reflex-chain model can be refuted, in both forward and backward locomotion as well as during swimming and crawling behaviors. We show that information theory applied to animal behavior can yield insights into the neural control of behavior.

C. elegans | information theory | locomotion | motor control

1 **H**ow the nematode *C. elegans* moves in a well-executed serpentine fashion is still unknown despite a detailed anatomical knowledge, connectome and genetic access to each of its 302 neurons (1, 2). The body motor system of *C. elegans* consists of overlapping 95 body wall muscle cells that ring the body and 75 body motor neurons grouped into 12 similar neuromuscular units running down the body (3). Two main models exist for *C. elegans* locomotion: a reflex-chain model where the dorsoventral undulations of the head set up an oscillatory pattern that propagates down the body via connections between adjacent neuromuscular units and biomechanical linkage, and an alternative active posture model where the sinusoidal body posture along the entire body is effected by active neural control not solely deriving from lateral neuromuscular signaling from the head to tail (Fig 1a). The earliest computer simulations of *C. elegans* movement were based on a reflex-chain model, and more recent simulations based on proprioceptive reflex chains recapitulate aspects of *C. elegans* movement (4–7). Worms crawl on their side with a smoothly propagating sinusoidal undulation with little body slippage outside of the sinusoidal path they trace out on their crawling surface; we surmise that the appearance of a smooth and consistent traveling wave inspired the reflex-chain model.

24 An alternative model, which we term the active posture model, posits that worm motion is driven by multiple sites of centrally coordinated neural signals along the body. (Fig. 1a). 25 These signals may be produced by a pattern generator (CPG) 26 consisting of one more cells. Recently, rhythmically active 27 groups of neurons for forward and backward locomotion have 28 been identified (8–12), but whether these groups of neurons 29 represent autonomous CPGs is still to be resolved.

Results

33 **Cross-correlation of postural angle time series reveals non-monotonic noise accumulation down the body.** To generate 34 quantitative worm movement data, we recorded high resolution 35 videos of worms crawling on an agar surface using a

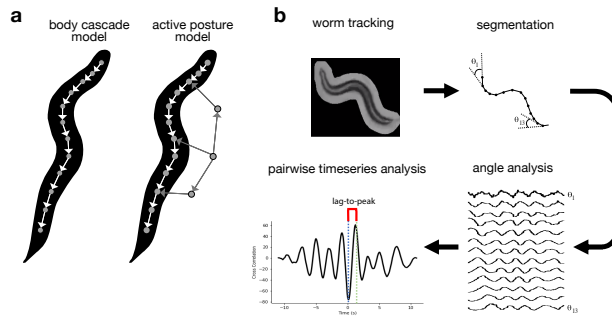


Fig. 1. Locomotion models and analysis overview. a. Schematics of the reflex-chain model (left) versus the active posture model (right). b. Overview of analysis of worm movement. Sustained bouts of forward locomotion were tracked, worm skeletons were segmented, and the worm tangent angles were plotted versus time for each segment. Finally, pairwise measures – time lag to peak cross-correlation, peak absolute cross-correlation, and mutual information were calculated for all joint angle pairs.

37 custom-built motorized-stage microscope and image-based tracking software system (13) and performed video analysis 38 (14) to silhouette and segment the worms. We then extracted 39 time series of the postural tangent angles between each of 40 13 body segments (Fig. 1b). As expected, these time series 41 resembled a series of phase-lagged noisy sinusoids. Performing 42 analysis with a finer discretization of body segments did not 43 change the key findings.

44 The sinusoidal appearance of the signals suggested that 45 cross-correlation analysis would be revealing. The cross- 46 correlation of two closely related sinusoidal signals in the 47 presence of noise consists of a set of peaks of decaying 48 magnitude (Fig. 1b). The x-coordinate of the peak of the 49 cross-correlation provides an estimate of the time lag of the 50 signals. The maximum absolute value of the cross-correlation 51 provides a scalar estimate of the relatedness of the signals 52 measured at the most favorable relative time delay, and it is 53 reduced by the amount of noise present in the transformation 54 between the signals. To simulate the undulations of forward 55 locomotion under the reflex-chain model, we created a sine wave 56 to represent head postural angle time series, added noise and a 57 phase delay to the signal to generate the posteriorly adjacent 58 postural angle time series, and iterated this procedure down 59 the body.

60 We computed the cross-correlation between each body joint 61 angle with respect to the anterior-most (head) joint angle 62

JW wrote the code for the project and performed the experiments. JW and SK worked together on all other aspects of the project, including conceptualization, data analysis, and writing.

No conflicts of interest.

Correspondence should be addressed via e-mail to: saul.kato - at - ucsf.edu

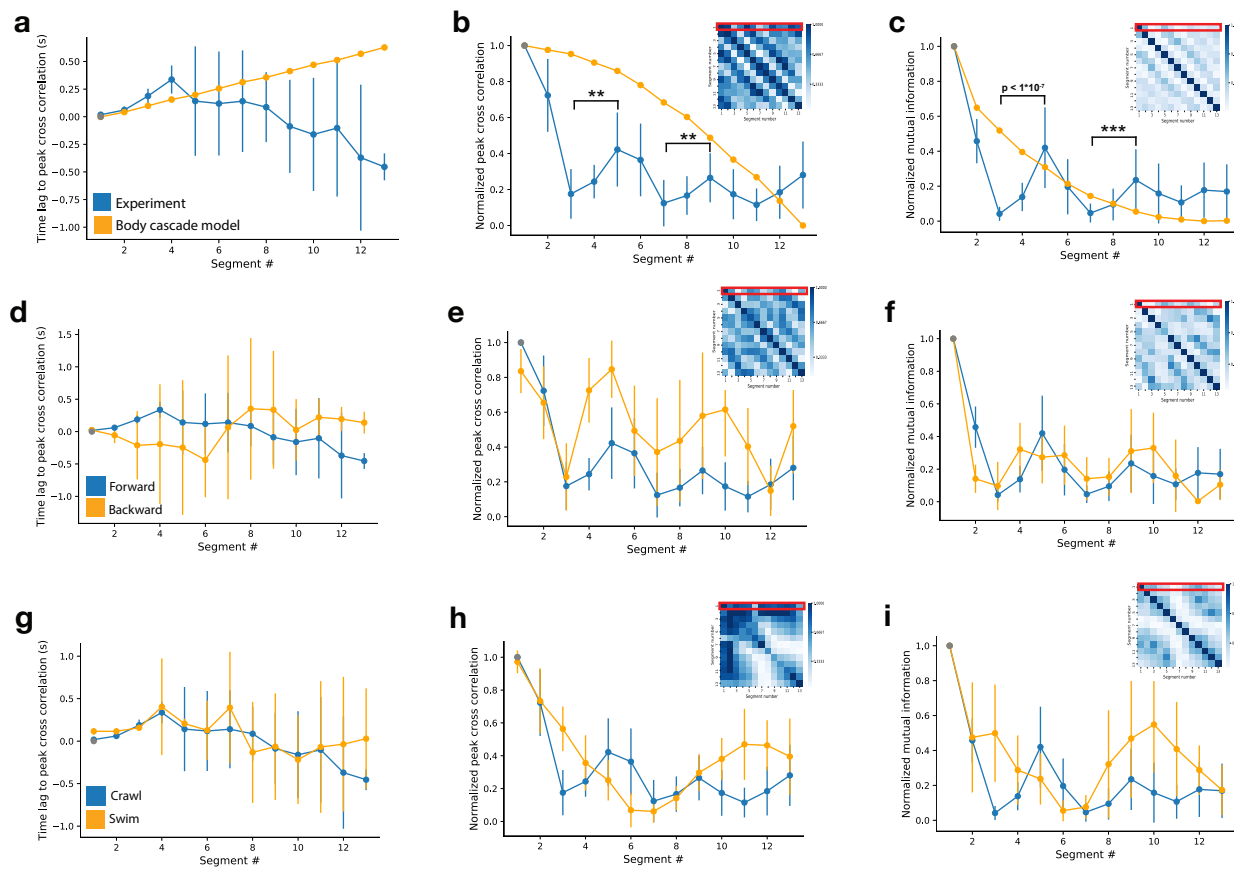


Fig. 2. a-c: Postural angle time series relationships during forward locomotion. a. Time lag to the peak cross correlation vs angle # calculated for the reflex-chain model (orange) and wild-type worms (blue) for forward locomotion, $n=10$. b. Heat map shows peak abs. cross-correlations computed between all angle pairs; first row is shown in the larger plot. Note that the experimental data is non-monotonic, in contrast to the model. (Segment 5 — segment 3 and segment 9 — segment 7, random sampling with replacement, $**p<0.01$) c. Mutual information plotted between all angles in the inset heatmap, with the mutual information relative to the head angle plotted. (Segment 5 — segment 3 and segment 9 — segment 7, random sampling with replacement, $***p<0.001$) d-f: **Forward versus backward crawling.** d. Time lag to peak cross-correlation for forward (blue) and backward (orange) locomotion (compared to the head angle for forward and tail angle for backward), $n=9$ worms. e. Peak abs. cross-correlation normalized to the head angle for forward (blue) and tail angle for backward (orange). f. The peak mutual information normalized to the head angle for forward (blue) and tail angle for backward (orange). g-i: **Forward crawling versus swimming.** g. Time lag to peak cross-correlation for crawling (blue) and swimming (orange) locomotion compared to the anterior-most segment. $n=10$ worms for each group. h. Peak abs. cross-correlation for crawling (blue) and swimming (orange) locomotion normalized to the anterior-most segment. i. The mutual information for crawling (blue) and swimming (orange) locomotion normalized to the anterior-most segment.

63 during this simulated pattern of forward locomotion (Fig. 1b). As expected, in the reflex-chain model simulation, the
 64 time lag to peak cross-correlation with respect to the first
 65 segment time series increased monotonically, and the peak
 66 absolute cross-correlation with respect to the first segment time
 67 series decreased monotonically with increasing segment number
 68 (Fig. 2a,b). We then performed the same analysis of our
 69 experimental data. For this analysis, we selected contiguous
 70 time series sections when the animal was crawling forward
 71 and not turning. In our experimental worms, we did not
 72 observe a stably increasing time lag to peak cross-correlation
 73 (Fig. 2a), and strikingly, we observed a strong breaking of
 74 monotonicity in the peak absolute cross-correlation (Fig. 2b).
 75 There were local minima in the peak absolute cross-correlation
 76 of angle pairs (1,5) and (1,9). This deviation from monotonicity
 77 suggests that the reflex-chain model is a poor fit to experiment.
 78 However, there was trial-to-trial variability in the pattern of
 79 peak correlations and time lag; thus, we sought a more robust
 80

measure of information transmission.

81

Mutual information suggests centrally coordinated posture control. A central theorem of information theory is the *data processing inequality*: a propagating signal can only lose, and not gain information from transmission from point to point, due to the accumulation of noise (15). If a worm moved according to the reflex-chain model, the mutual information between the head joint angle and each successive body angle would monotonically decrease (Fig. 2b, c). However, we found a strong experimental deviation from monotonic information loss. The two local maxima of the mutual information relative to angle 1 occur at the same angle numbers (5 and 9) as the two local maxima of the peak absolute cross-correlation, suggesting that active postural control may be transmitted to the periphery through two specific points. We also measured the mutual information between all angle pairs (Fig. 2c, inset).

82
 83
 84
 85
 86
 87
 88
 89
 90
 91
 92
 93
 94
 95
 96

97 **Forward crawling, backward crawling, and swimming are**
98 **under centrally coordinated postural control.** We extended
99 our analysis to backwards locomotion, in this case using the
100 posterior-most (tail) angle as angle 1. *C. elegans* backwards lo-
101 comotion is shorter in bout duration and crawling length than
102 forwards locomotion, so we employed shorter time windows
103 than those used for forward locomotion. Similar to forward
104 locomotion, we found a non-monotonic peak absolute cross-
105 correlation and non-monotonic mutual information (Fig. 2e,
106 f). The peak absolute cross-correlation has local maxima for
107 angle pairs (1,5) and (1,10) (Fig. 2e, f). A reflex-chain model
108 can thus be rejected for both directions of crawling, and both
109 appear to coordinate control at two points along the body.

110 We then analyzed worm swimming. It has been argued
111 that *C. elegans* swimming and crawling represent distinct
112 neural control patterns (16) rather than solely the result of
113 biomechanical influence of a changing physical substrate. We
114 found the time-lag to absolute cross-correlation to be non-
115 monotonic but, in contrast to the crawling state, the peak
116 absolute cross-correlation has only one, rather than two local
117 maxima, suggesting a different mode of central coordination.
118 (Fig. 2g, h). The reflex-chain model can be rejected for
119 swimming worms as well as crawling worms.

120 Discussion

121 We claim that the reflex-chain model of worm movement
122 is inconsistent with fine analyses of behavioral data. Our
123 data suggests there are two body locations where central
124 coordination reaches the periphery. With higher resolution
125 video recordings, detailed anatomical registration of neural and
126 neuron-to-muscle connectivity data from the worm connectome
127 could suggest particular neurons and connections responsible
128 for centrally coordinated posture control.

129 Our data is consistent with recent loss-of-function studies.
130 One study showed that forward-rhythm undulations persist in
131 posterior body segments even when anterior body segments
132 are paralyzed (8). Another study found that when anterior A
133 motor neurons were ablated, it did not prevent the propagation
134 of reversal waves in posterior body segments (9). In addition
135 to recent studies suggesting the presence of neural oscillators,
136 there is also evidence for lateral information transmission be-
137 tween adjacent neuromuscular units (17). If there are multiple
138 CPG groups driving locomotion, our data suggest that they are
139 strongly coupled. We hypothesize that coordinated oscillatory
140 postural control signals reach the neuromuscular periphery
141 at two specific points along the body, bypassing intervening
142 neuromuscular units. These signals are shaped into a spatially
143 smooth traveling body waveform by lateral neuromuscular
144 signal transmission and further smoothed by biomechanical
145 linkage.

146 We assume that there is not severe segment-to-segment
147 heterogeneity in the noise accumulated during the local biome-
148 chanical transformation from muscle to body bend angle; if
149 this transformation noise were both strong and wildly differ-
150 ent along the body, it could undermine our interpretation of
151 the non-monotonicity of our measures. However, we find this
152 unlikely given the robustness of the results and lack of an
153 intuition as to how such heterogeneity might occur.

Materials and Methods

We recorded videos of wild-type (N2) worms using a custom track-
154 ing microscope and TierpsyTracker software (13, 14). We manu-
155 ally identified bouts of forward crawling, backward crawling, and
156 swimming. Analysis code is available at <https://github.com/focolab/>
157 worm-locomotion-control and was written in python.
158
159

ACKNOWLEDGMENTS. SK is funded by the NIGMS
(R35GM124735), the Alfred Sloan Foundation, and the Weill Neuro-
160 hub. The CGC is funded by NIH Office of Research Infrastructure
161 Programs (P40 OD010440).

1. Izquierdo EJ, Beer RD (2016) The whole worm: brain–body–environment models of *C. elegans*. *Current Opinion in Neurobiology* 40:23–30. Systems neuroscience. 164
2. Gjorgjieva J, Biron D, Haspel G (2014) Neurobiology of caenorhabditis elegans locomotion: Where do we stand? *BiScience* (64,6):476 – 486. 165
3. Haspel G, O'Donovan MJ (2011) A perimotor framework reveals functional segmentation in 166 the motoneuronal network controlling locomotion in caenorhabditis elegans. *The Journal of 167 Neuroscience* (31(41)):14611 – 14623. 168
4. Niebur E, Erdős P (1991) Theory of the locomotion of nematodes: Dynamics of undulatory 169 progression on a surface. *Biophysical Journal* (60):1132 – 1146. 170
5. Bryden J, Cohen N (2008) Neural control of caenorhabditis elegans forward locomotion: the 171 role of sensory feedback. *Biological Cybernetics* 98:339 – 351. 172
6. Karbowiak J, Schindelman F, Cronin CJ, Seah A, Sternberg PW (2008) Systems level circuit 173 model of c. elegans undulatory locomotion: mathematical modeling and molecular genetics. 174 *Journal of Computational Neuroscience* 24:253 – 276. 175
7. Gleeson P, Lung D, Grosu R, Hasan R, Larson S (2018) c302: a multiscale framework for 176 modelling the nervous system of caenorhabditis elegans. *Phil. Trans. R. Soc. B* 373:20170379. 177
8. Fouad AD, et al. (2018) Distributed rhythm generators underlie caenorhabditis elegans forward 178 locomotion. *eLIFE* (7):e29913. 179
9. Gao S, et al. (2018) Excitatory motor neurons are local oscillators for backward locomotion. 180 *eLife* (7):e29915. 181
10. Qi YB, et al. (2013) Hyperactivation of b-type motor neurons results in aberrant synchrony of 182 the caenorhabditis elegans motor circuit. *The Journal of Neuroscience* (33(12)):5319 – 5325. 183
11. Olivares EO, Izquierdo EJ, Beer RD (2017) Potential role of a ventral nerve cord central 184 pattern generator in forward and backward locomotion in caenorhabditis elegans. *Network 185 Neuroscience* (2,3):323 – 343. 186
12. Xu T, et al. (2018) Descending pathway facilitates undulatory wave propagation in caenorhab- 187 ditis elegans through gap junctions. *PNAS* (115,19):E4493 – E4502. 188
13. Yemini El, Brown AEX (2015) Tracking single c. elegans using a usb microscope on a motorized 189 stage. *Methods in Molecular Biology* (1327):181 – 197. 190
14. Javer A, et al. (2018) An open-source platform for analyzing and sharing worm-behavior data. 191 *Nature Methods* (15):645 – 646. 192
15. Cover T (2012) *Elements of information theory*. (John Wiley & Sons). 193
16. Pierce-Shimomura JT, et al. (2008) Genetic analysis of crawling and swimming locomotory 194 patterns in c. elegans. *PNAS* (105,52):20982–20987. 195
17. Wen Q, et al. (2012) Proprioceptive coupling within motor neurons drives c. elegans forward 196 locomotion. *Neuron* (76,4):750 – 761. 197
18. 198
19. 199